Proceedings of the ASME 2016 35th International Conference on Ocean, Offshore and Arctic Engineering
OMAE2016
June 19-24, 2016, Busan, South Korea

OMAE2016-54973

OPTIMIZATION OF FLOATING OFFSHORE WIND ENERGY SYSTEMS USING AN EXTENDED PATTERN SEARCH METHOD

Caitlin Forinash
School of Mechanical, Industrial, and Manufacturing Engineering
Oregon State University
Corvallis, Oregon, United States
forinasc@oregonstate.edu

Bryony DuPont
School of Mechanical, Industrial, and Manufacturing Engineering
Oregon State University
Corvallis, Oregon, United States
Bryony.DuPont@oregonstate.edu

ABSTRACT

An Extended Pattern Search (EPS) approach is developed for offshore floating wind farm layout optimization while considering challenges such as high cost and harsh ocean environments. This multi-level optimization method minimizes the costs of installation and operations and maintenance, and maximizes power development in a unidirectional wind case by selecting the size and position of turbines. The EPS combines a deterministic pattern search algorithm with three stochastic extensions to avoid local optima. The EPS has been successfully applied to onshore wind farm optimization and enables the inclusion of advanced modeling as new technologies for floating offshore wind farms emerge. Three advanced models are incorporated into this work: (1) a cost model developed specifically for this work, (2) a power development model that selects hub height and rotor radius to optimize power production, and (3) a wake propagation and interaction model that determines aerodynamic effects. Preliminary results indicate the differences between proposed optimal offshore wind farm layouts and those developed by similar methods for onshore wind farms. The objective of this work is to maximize profit; given similar parameters, offshore wind farms are suggested to have approximately 24% more turbines than onshore farms of the same area. EPS layouts are also compared to those of an Adapted GA; 100% efficiency is found for layouts containing twice as many turbines as the layout presented by the Adapted GA. Best practices are derived that can be employed by offshore wind farm developers to improve the layout of platforms, and may contribute to reducing barriers to implementation, enabling developers and policy makers to have a clearer understanding of the resulting cost and power production of computationally optimized farms; however, the unidirectional wind case used in this work limits the representation of optimized layouts at real wind sites. Since there are currently no multi-turbine floating offshore wind farm projects operational in the United States, it is anticipated that this work will be used by developers when planning array layouts for future offshore floating wind farms.

NOMENCLATURE

P	Power
ρ	Air density
A	Rotor swept area
r_r	Rotor radius
U_0	Free stream wind speed
U	Wind speed in wake
C_p	Power coefficient
N	Number of wind turbines in farm
c_f	Capacity factor
t	Total number of operational hours
POE	Price of Electricity
P_{tot}	Total power production of all turbines
r_1	Width of wake behind rotor
y	Distance downstream from rotor
$\propto$	Entrainment constant
z	Hub height
z_0	Surface roughness
P_{rated}	Rated power of a wind turbine
$P_{rated,farm}$	Rated power of the entire wind farm
d_t	Total length of inter-array cabling
d_s	Distance of farm from shore
h	Water depth
r	Operating fee rate
α_h	Power law exponent
u_r	Reference wind speed
z_r	Reference height

INTRODUCTION

As population continues to grow and Americans increasingly use technological and powered products, it is predicted that the demand for power in the United States will increase by as much as 29% by the year 2040 [1]. Meeting this need will require not only the advancement of existing renewable energy systems (such as onshore wind farms and solar arrays), but also the development of novel renewable energy systems.

The United States Department of Energy (DOE) estimates that approximately 54 MW of offshore wind power will be installed off the coasts of the U.S. by 2030 [2]. While many proposed farms are to be located in the shallower waters off the northeast and mid-Atlantic states, it is imperative to capitalize on the large wind resource off the deep-water west coast of the United States, whose predicted resource totals more than 900 GW [3].

The vast majority of offshore wind projects have been embedded wind farms that use either bottom-fixed monopoles, jackets, or gravity-based foundations to support wind turbines [4]. These embedded structures are best used for water depths ranging from 10 to 15 meters [5], although the costs do not become prohibitive until a water depth of 30 meters [6]. Extra long (XL) monopoles may be feasible in water depths up to 40 meters, and deep-water jackets can support turbines in water depths of 30-60 meters [7]. The waters off the coasts of the leading European countries, as well as the North American east coast, lend themselves well to these types of turbines since the waters are shallow and the bathymetry is gentle. However, the North American west coast has a sharper bathymetry, making the use of embedded offshore wind turbines impractical.

Expanding offshore wind technologies into deeper water increases the resource area as well as the total available wind resource, since wind speeds are higher and more predictable over deep waters [8]. Since embedded platforms are not possible in deep ocean waters, other options must be considered. There are many proposed floating platform designs; three current platform designs are spar-buoy, tension leg-platform (TLP), and semi-submersible. HyWind is the first full-scale floating turbine; it is located off the coast of Norway in 200-meter water depth and has been grid-integrated since 2010. It is a spar-buoy, long-ballast column design. Another floating wind turbine, the WindFloat semi-submersible platform designed by the US company Principle Power, has a 2 MW project located 5 kilometers off the coast of Portugal [9]. It has been generating electricity since 2012 and has produced nearly 10 million kWh since its implementation. An additional three or four 6-8 MW floating turbines are to be installed by 2017 at the Portugal site [10].

The US west coast has made progress in recent years with Oregon leading the industry in offshore wind development. According to the National Renewable Energy Laboratory, at 12 miles off the Oregon Coast there is a potential wind resource of nearly 220 GW [11]. As of May 2014, a new project has been commissioned by the DOE, WindFloat Pacific, which will develop 30 MW of wind power in deep waters off the coast of Coos Bay, Oregon [12].

The high cost of offshore wind farms can be prohibitive; in addition, structures in water have many inherent complications. Offshore turbines are often difficult to maintain due to extreme weather conditions; if a turbine were to malfunction during a stormy duration of the year it could be many weeks before a team could fix it. There are also higher installation and maintenance costs for offshore turbines, although it is expected that the higher resources and dispatchability of the wind energy potential will compensate these costs. For the offshore wind industry to thrive, research must be conducted that will help lower the costs of offshore wind power installations. Optimizing the layouts such that power production is maximized and cost is minimized will help make offshore wind power installations more feasible and affordable.

OFFSHORE WIND FARM OPTIMIZATION

Previous research in offshore wind farm optimization has been conducted, though these methods are generally applied to embedded, non-floating platforms. Elkinton et al. [13] presented an offshore wind farm optimization method with power-maximization and cost-minimization models that enabled a Levelized Cost of Energy (LCOE) objective function for bottom-fixed wind farms. These models can be employed within any heuristic optimization algorithm as applied to bottom-fixed offshore wind farms, and multiple heuristic algorithms for combinatorial optimization have been proposed [14]. Pérez et al. developed a two-step sequential procedure that also can be applied to any heuristic optimization algorithm [15]. The first step is a heuristic method to set a random initial layout, and the second step includes nonlinear mathematical program techniques to find local optima. The technique was applied to the Alpha Ventus offshore wind farm and showed an increase in AEP of 3.76%. Genetic Algorithms and Greedy Heuristic algorithms were found to be the most viable for the offshore wind farm layout problem, as compared to data from an existing offshore wind farm; however, Extended Pattern Search algorithms have not previously been explored [14].

Genetic Algorithm (GA) approaches have been the most common method in offshore wind farm optimization. Gao et al. optimized aligned, staggered, and scattered layouts [16]. Scattered layouts proved to be most optimal, and were optimized using a Multi-Population GA [17]. Réthoré et al. applied a multi-fidelity model approach to an offshore test case at Middelgrunden, Denmark [18]. The multi-fidelity approach ran 1000 iterations of a Simple GA followed by 20 iterations of a Sequential Linear Programming method and includes fatigue costs within the framework. Liu and Wang use an Adaptive GA, which replaces the random crossovers of conventional GA's with location swaps [19]. GA's are stochastic and perform well for layout optimization applications; however, GA's traditionally use a discretized space and do not allow for continuous placement , and therfore efficient packing, of turbines.

In Liu and Wang's research, three wind cases were used: two unidirectional cases at 12 m/s and 20 m/s, and a multi-directional, multi-speed case [19]. A 16 turbine wind farm for Case 1 (unidirectional, 12 m/s wind speed) has 100% efficiency such that all turbines in the array completely avoid wake interactions of upstream turbines. This work compares the efficiency of wind farms generated using an Extended Pattern Search (EPS) approach to the efficiency of the 16 turbine wind farm generated by the Adapted GA for the unidirectional wind case.

Additional offshore wind farm optimization methods have also been explored. Rivas et al. applied a Simulated Annealing algorithm using actual test site data, including the Horns Rev offshore wind farm [20]. Results show an increased AEP of 1% over the actual layout of the Horns Rev wind farm. Ituarte et al. developed a Viral Based optimization algorithm to mimimize cost of energy (COE) [21]; the 26 turbine layout reduces the COE as compared to Mosetti et al.'s 30 turbine onshore layout optimized using a Genetic Algorithm [22]. Salcedo-Sanz et al. used a Coral Reefs Optimization algorithm that showed improvement over Evolutionary, Differential Evolution, and Harmony Search algorithms [23]. One optimization method has been applied to floating offshore wind farms. Rodrigues et al. used an evolutionary optimization strategy in a nested configuration called Covariance Matrix Adaption (CMA-ES) to optimize a floating offshore wind farm comprised of IDEOL platforms [24,25]. The CMA-ES is used to optimize the anchoring locations of the wind turbine position within the mooring lines. The tool can be used to optimize wind farms composed of either stationary or moveable floating turbines.

This work explores the application of an Extended Pattern Search (EPS) algorithm to offshore wind farm layout optimization while expressly considering the challenges of deep-water installations, i.e. the use of floating wind turbine platforms. This optimization method explores (1) minimizing the cost of installation and operations and maintenance costs and (2) maximizing power development to drive down the cost of floating offshore wind farms. The EPS is inherently able to accommodate the varying numerical modeling of the factors associated with floating offshore wind farm array optimization to find optimal array positioning solutions. Research using the EPS has shown to significantly improve the performance of onshore wind farms [26–29]. Preliminary results will inform researchers of the economic feasibility of installing floating offshore wind farms using optimized array layouts.

METHODOLOGY

1. EXTENDED PATTERN SEARCH

An Extended Pattern Search (EPS) is a moderately stochastic non-gradient search method that traverses the search space in a series of user-defined moves. The EPS combines a deterministic pattern search algorithm with stochastic extensions. This work uses three extensions that will be explained in further detail: randomized initial layout, randomized search order, and a popping algorithm. The added stochasticity allows for the EPS to avoid settling on local optima. EPS methods enable the inclusion of advanced modeling as new technologies for offshore wind farms are introduced. Modeling advances must be incorporated into the EPS to account for the challenges of deep-water installations. These modeling advances include cost, power development, and wake propagation and interaction models.

The pseudocode shown in Fig. 1 shows how the three extensions are integrated into the pattern search, and can be used to understand the functionality of the EPS described in this work.

1.1 PATTERN SEARCH

Pattern search algorithms are a type of direct search algorithm. Direct search algorithms were introduced by Hooke and Jeeves for computing optimal solutions when classical methods are infeasible, such as the multi-modal floating offshore wind turbine array placement problem [30]. Pattern search is a deterministic search method that does not require the calculation of derivatives [31]. Pattern searches are computationally inexpensive and, given the same starting point, will always converge upon the same solution.

A pattern search begins with an agent in an initial position and the objective is evaluated. The agent moves in the first search direction, positive x direction, at a user-defined step size. The objective is evaluated for the new location and compared to the original location. The pattern search is greedy, such that if the new location results in an improved global objective evaluation, the move is accepted and the new agent location is updated to the current location. However, if the objective evaluation at the new location is poorer than the original location, the agent will move back to the original location and try the next move. The second search direction is in the positive y direction. Again, the new location is evaluated and compared to the original location. If the objective evaluation is not improved, the pattern search will try the negative *x* direction, then the negative *y* direction. If none of the search directions result in an improved objective evaluation, the step size is reduced. The pattern search is repeated as described above until the step size has been reduced to a user-defined lower bound step size. Once the pattern search has been exhausted, the agents are considered to have reached stopping criterion.

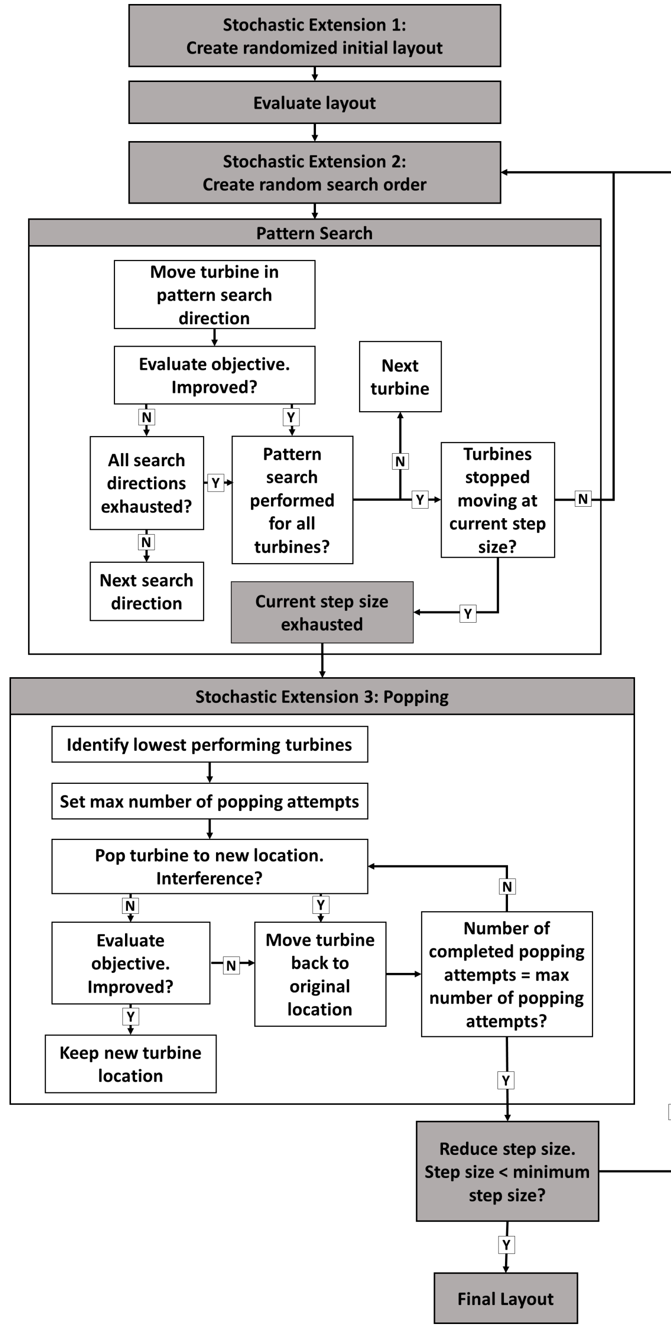

FIGURE 1: EPS PSEUDOCODE

1.2 STOCHASTIC EXTENSIONS

Yin and Cagan introduced an EPS for three-dimensional component layout optimization which can be applied to general layout problems [32]. The extensions demonstrated increased the likelihood of convergence on optimal solutions, at a rate much faster than a robust simulated annealing-based algorithm. The three stochastic extensions in this work add randomness to the pattern search, which helps the EPS to avoid converging on poor-performing local optima.

The first stochastic extension in the current EPS is randomized initial turbine position. When the EPS begins, all agents are placed into the search space at random locations such that the original layout is unique to each run. Turbines must be located at least five rotor radii from other turbines and they must be within the search space.

The second stochastic extension in the EPS is randomized search order. At the beginning of each new step size within the pattern search, the search order is randomized. The pattern search moves one agent at a time and evaluates the objective for the entire farm. The location of a single turbine affects the power production of other turbines within the farm. In order to avoid biasing particular agents, the order in which the turbines move must be randomized.

The third stochastic extension is the popping algorithm, which occurs so that the EPS does not settle on poor-performing local optima. Once a step size has been exhausted in the pattern search, the popping extension begins. A user-defined number of low-power turbines are "popped" to new locations within the search space. These new locations are random in the space and may overlap with other turbines. The new turbine locations are first evaluated for their proximity to other turbines. If the new location is not within five rotor radii of another turbine, the objective is evaluated for the new location. If the new location improves the overall objective evaluation, the new location is accepted. If it does not improve the objective evaluation, the turbine is moved back to its original location. The popping extension continues until all of the low-power turbines have been moved to new locations, or a user-defined maximum number of popping attempts has been reached. Once the popping algorithm is complete, the EPS continues onto the pattern search with a new, reduced step size.

1.3 OBJECTIVE FUNCTION

The purpose of this work is to provide a method for developers that will reduce the cost of installing a floating offshore wind farm. The objective function considers both the power production of the wind farm and the costs. The cost and power models will be described in further detail in the next section. The objective function is given in Equation 1.

$$Objective = Cost_{total} - (P_{tot} \times c_f \times POE \times t) \tag{1}$$

where $Cost_{total}$ is the total cost of the wind farm (Equation 6), P_{tot} is the total power produced (Equation 3), c_f is capacity factor, t is the total number of hours that the wind farm is operational, and POE is the price of electricity. The objective function is given in negative null form, meaning that optimal solutions occur when the objective function is minimized.

1.4 STOPPING CRITERIA

Due to the multi-modality and both discrete and continuous nature of the wind farm layout optimization problem and EPS, global convergence is not guaranteed. Instead, stopping criteria are defined to determine when the EPS has sufficiently exhausted potential layouts. The popping algorithm has two stopping criteria: either all low-performing turbines have been moved to new locations, or a user-defined maximum number of popping iterations has been reached. The stopping criterion for the EPS occurs after a user-defined minimum step-size pattern search has been exhausted.

2. POWER MODEL

In order to determine the profitability of a wind farm, the power production must be calculated. The power production equation (Eq. 2) is defined by Manwell et al. as [33]:

$$P = \frac{1}{2}\rho A U^3 C_p \tag{2}$$

where ρ is air density, A is rotor swept area, equal to $\pi {r_r}^2$, U is wind speed at the rotor, and C_p is the power coefficient. Equation 2 describes the cubic power curve between the cut-in wind speed, $u_{cut\text{-}in}$ and the rated wind speed, u_{rated}. For wind speeds below $u_{cut\text{-}in}$, the wind turbine is not producing power. For wind speeds between u_{rated} and $u_{cut\text{-}out}$, the power produced is equal to the rated power of the wind turbine. This work uses cut-in and rated wind speeds of 3 m/s and 11.5 m/s, respectively.

The power production model in the EPS includes a turbine geometry selection that selects turbine hub height and rotor radius for individual turbines. The turbine size model is based on a database of commercially-available three-bladed horizontal-axes wind turbines; this database has been extended to accommodate the larger geometries of offshore turbines. The turbine geometry selection is continuous but only allows for feasible geometry relationships for hub height and rotor radius based on existing manufactured turbine geometries. The turbine geometry selection has shown to improve the overall objective for onshore wind farms [29]. Hub height selection ranges from a minimum of 38 meters to a maximum of 135 meters.

The total power production of the wind farm is calculated as the sum of the power production for each individual turbine, as shown in Equation 3.

$$P_{tot} = \sum_{i=1}^{N} P_i \tag{3}$$

Increased values of P_{tot} result in better objective evaluations (Eq. 1). Equation 2 describes the power production of a wind turbine in free stream flow. The next section describes how to calculate power production when turbines are downstream of other turbines such that wake interactions occur.

2.1 WAKE PROPAGATION AND INTERACTION MODELING

The three dimensional wake model used in this work is derived from the PARK Model [34]. This simplified wake model is used to determine how wakes created by upstream turbines affect the wind environment at downstream turbines. Rotating blades extracting energy from the wind create a conical wake that propagates downstream. The wind speed is greatly reduced within the turbine's wake, as shown in Fig. 2. As the wake propagates, the reduced wind speed recovers asymptotically to the ambient wind speed downstream.

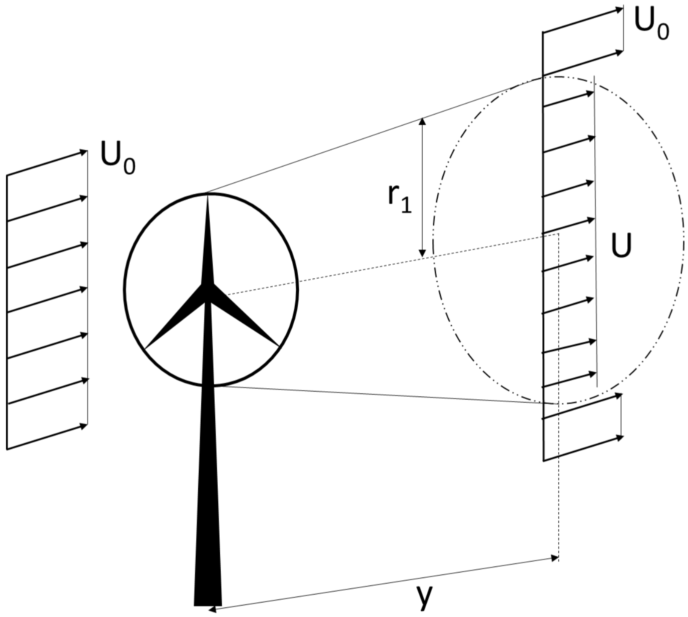

FIGURE 2: THREE DIMENSIONAL WAKE PROPAGATION

The width of the wake, r_1, and the wind speed, U, are proportional to the distance downstream from the rotor, y [26]. The free stream, or ambient, wind speed is denoted U_o. The effective wind speed at a downstream wind turbine is calculated in Equation 4. This value is the wind speed that is used in the power equation (Eq. 2):

$$U = U_o[1 - \frac{2}{3}\left[\frac{r_r}{r_r + \propto y}\right]^2] \quad (4)$$

where r_r is rotor radius, and $\propto$ is the entrainment constant, which is calculated in Equation 5:

$$\propto = \frac{0.5}{\ln\left({}^{z}/_{z_0}\right)} \quad (5)$$

where z is the hub height and z_0 is the surface roughness. A turbine may be affected by multiple wakes, as shown in Fig. 4.

The equations for the effective wind speed at a downstream rotor affected my multiple wakes as well as overlapping wakes are given by DuPont et al [26,29]. For rotors in multiple, non-overlapping wakes, the wind speed is calculated as a function of the percentage of the rotor swept area in each wake. Calculating wind speed due to overlapping wakes is more complex; a 49 point discretized mesh is superimposed over the rotor swept area, and the wind speed is calculated at each discrete location. The average effective wind speed across these locations is then considered as the effective wind speed at the turbine.

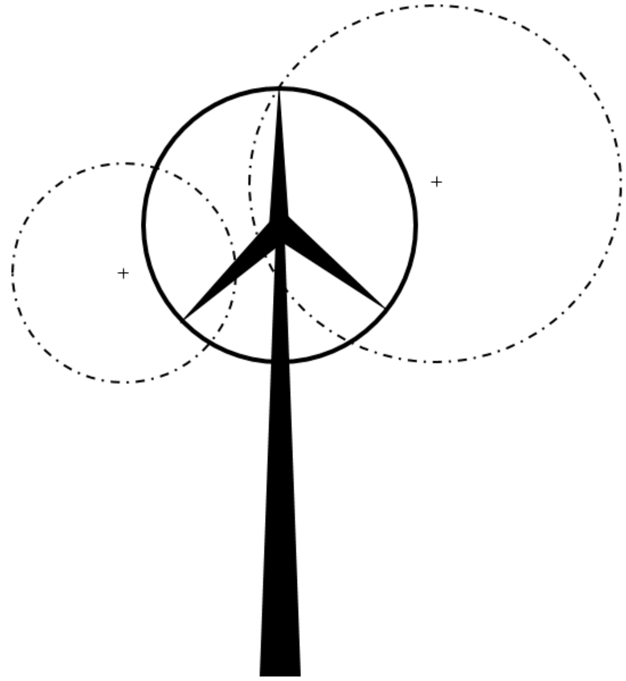

FIGURE 3: MULTIPLE WAKES INTERACTING WITH A ROTOR SWEPT AREA

3. COST MODEL

The cost of a floating offshore wind farm is the summation of the capital, cabling, mooring, annual O&M, substation, installation, and leasing costs. Equation 6 shows the formulation for the total cost.

$$Cost_{Total} = Cost_{capital} + Cost_{cabling} + Cost_{mooring} + Cost_{O\&M} + Cost_{sub} + Cost_{installation} + Cost_{operating\ lease} \quad (6)$$

3.1 TURBINE AND PLATFORM CAPITAL COST

The capital cost includes the costs of both the wind turbine and the WindFloat floating platform [9]. Castro-Santos references the REpower 5.075 MW wind turbine [35] that requires a semisubmersible floating platform of mass 695,985 kg [36]. The cost of this wind turbine is \$1.32 million/MW. The cost of the semisubmersible platform is \$575.65/ton, or \$400,644 for a platform supporting a 5.075 MW turbine. The total cost of the 5.075 MW turbine and semisubmersible platform is \$1.48 million/MW, as shown in Eq. 7:

$$Cost_{capital} = P_{rated,farm} \times \$1.48\ million \quad (7)$$

where $P_{rated,farm}$ is the rated power of the entire farm in MW, given in Eq. 8:

$$P_{rated,farm} = \sum_{i=1}^{N} P_{rated,turbine,i} \quad (8)$$

where N is the number of turbines in the farm and $P_{rated,turbine}$ is the rated power of each turbine.

3.2 CABLING COST

The cabling system for a floating offshore wind farm is comprised of two types of cables: inter-array cables and export cables. Inter-array cables connect turbines in the array to a single location, such as a turbine at the front of the farm. The power is sent to an onshore substation via an export cable.

The cost of inter-array cabling is \$307,000/km; Equation 9 calculates the cost for the inter-array cabling of the entire farm [37]:

$$C_{inter\text{-}array} = d_t \times \$307{,}000 \quad (9)$$

where d_t is the total length of the inter-array cables. The cost of the export cables relies on the distance between the substation and shore, d_s, in kilometers. The cost of export cabling is \$492,000/km; Equation 10 gives the cost for the export cabling [37].

$$Cost_{export} = d_s \times \$484{,}000 \quad (10)$$

Equation 11 determines the total cost of cabling, which is the sum of the inter-array and export cabling costs.

$$Cost_{cabling} = Cost_{inter\text{-}array} + Cost_{export} \quad (11)$$

3.3 ANCHORING AND MOORING COST

The equations for the cost of anchoring and mooring are derived from work by both Castro-Santos et al. [38,39] and Myhr et al. [37]. Castro-Santos et al. considers 21 5.075 MW turbines on semisubmersible floating platforms off the Galician Coast in Northern Spain [39]. The WindFloat is anchored to the seafloor using drag embedment anchors [40]. The total manufacturing cost for each anchor is \$9,943, or \$39,772 for four anchors. Myhr considers a WindFloat moored in 200 meter water depth (h), requiring 200 meters of chain mooring and 2640 meters of steel wire [37]. The chain costs \$274/meter and the steel wire costs \$49.32/meter. As water depth changes, the length of a single chain is equal to the water depth, which will cost \$274/meter of water depth, or \$1096/meter of water depth for 4 lines. The length of the steel wire is constant at 2640 meters, which cost \$520,820 for four lines. Equation 12 calculates the total anchoring and mooring cost for the wind farm, assuming four lines are attached to the WindFloat platform [40].

$$C_{mooring} = N \times (\$39{,}772 + \$520{,}820 + \$1{,}096 \times h) \quad (12)$$

3.4 ANNUAL O&M COST

This work uses the O&M cost suggested by the Jobs and Economic Development (JEDI) Model for Offshore Wind Farms [41]. The JEDI Model uses an annual cost for O&M of \$133/kW for an offshore wind farm. Total O&M cost in the JEDI model is a function of the size of the wind farm ($P_{Rated,Farm}$) and the length of the project in years (t), given in Equation 13.

$$C_{O\&M} = \$133 \times P_{Rated,Farm} \times t \quad (13)$$

3.5 SUBSTATION COST

Two options are available for substation cost: (1) a floating offshore substation and (2) a traditional onshore substation. The offshore substation cost includes both the manufacturing cost and installation cost of a floating offshore substation. According to Myhr, the capital cost for a 500 MW offshore substation is \$177.24 million, and the installation cost is \$20.39 million [37]. For a 1000 MW substation, the capital cost is \$297.81 million and the installation cost is \$31.24 million. Equation 14 calculates the total capital and installation cost for a floating offshore substation as a function of the rated power of each wind turbine:

$$Cost_{sub} = \left(\$262840 \times P_{rated,farm}\right) + \$66{,}210{,}000 \quad (14)$$

where $P_{rated,farm}$ is in megawatts.

Onshore substation costs are based on real projects for substations built for wind farms and solar farms [42]. The baseline cost of a substation is \$2 million, with costs increasing linearly as the size of the farm grows, as shown in Equation 15.

$$Cost_{sub} = \$20{,}000 \times P_{rated,farm} + \$2{,}000{,}000 \quad (15)$$

According to the research used to develop the substation cost model, offshore substations are less economically feasible than onshore substations. As such, it is assumed that onshore substations will be used for the wind farms developed through this work; the cost of these substations is given in Eq. 15.

3.6 INSTALLATION COST

Castro-Santos identifies installation costs for the wind turbine, platform, mooring and anchoring, electrical, and commissioning (Eq. 16) [36].

$$C_{installation} = \$977{,}620 \times N \quad (16)$$

3.7 LEASING COST

The Bureau of Offshore Energy Management (BOEM) is in charge of regulating and leasing Outer Continental Shelf (OCS) area; their roles are to coordinate with all involved federal agencies, states, and local governments in order to ensure development is safe and environmentally-responsible, as well as obtain fair return for issued leases and grants [43]. A lessee begins paying "operating fees" once commercial generation of electricity has begun. Equation 17 can be used to calculate the cost of the operating lease [44]:

$$C_{operating\ lease} = P_{rated,farm} \times 8760 \times c_f \times COE \times r \times t \quad (17)$$

where 8760 is the total number of hours in a year, c_f is the capacity factor (0.4); COE is the annual average wholesale electric power price, r is the operating fee rate (equal to 0.02 for the first 8 years of operation, and 0.04 for the rest of the lease), and t is the length of the lease in years [44].

3.8 OTHER COST CONSIDERATIONS

The decommissioning cost is assumed to be negligible and will not be included in this model [36]. This work does not optimize the layout of mooring or inter-array cabling. The farm layouts determined from this work will inform optimal mooring and cabling configurations in future research, to further drive down costs.

3.9 ONSHORE COST MODEL

The optimized offshore layouts are compared to onshore layouts with similar parameters. The cost model for the onshore wind farm model is based on the polynomial cost surface as a function of rotor radius and hub height by DuPont et al [26].

4. PROBLEM FORMULATION

The wind case used in this work is unidirectional, single wind speed as shown in Fig. 4. The free stream wind speed is constant, approaching from the bottom of the field. For the comparison of the onshore and offshore layouts, the wind speed is 10 m/s; for the comparison of the EPS and Adapted GA, the wind speed is 12 m/s. The layouts are optimized within a 4000 m by 4000 m flat space. Water depth is 200 m and the farm is 30 kilometers from shore. The life of the farm is 20 years.

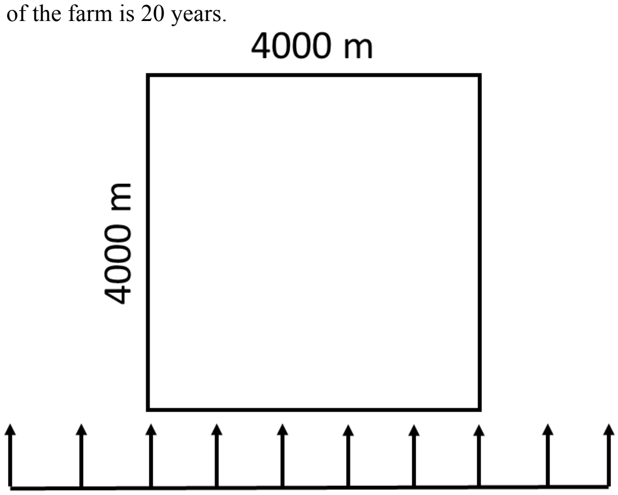

FIGURE 4: UNIDIRECTIONAL WIND CASE

The offshore layouts are compared to onshore layouts of the same size and wind speed. Surface roughness for onshore wind farms over a fallow field has an experimental value of $z_0 = 0.03$ meters, whereas the surface roughness of a calm open sea has an experimental value of $z_0 = 0.0002$ meters [33]. The wind profile power law is (Eq. 18):

$$\frac{u}{u_r} = (\frac{z}{z_r})^{\alpha_h} \tag{18}$$

where u_r and z_r are reference wind speed and heights, respectively. The power law exponent is $\alpha_h = 0.11$ for most offshore locations and stability conditions [3,45]. The onshore power law exponent is $\alpha_h = 0.1$ (unstable), $\alpha_h = 0.15567$ (neutral), and $\alpha_h = 0.2$ (stable) [26].

The number of popping attempts is set to 1000 for the poorest performing 10 turbines at each step size. Table 1 includes all parameters for the onshore and offshore wind layouts.

TABLE 1: OFFSHORE AND ONSHORE WIND FARM PARAMETERS

	Offshore	Onshore
Wind Speed	10 m/s	10 m/s
Farm Length	4000 m	4000 m
Water Depth	200 m	----
Life of Farm	20 years	20 years
Distance from Shore	30 km	----
Surface Roughness	0.0002 m	0.03 m
Power law exponent	0.11	0.1 (unstable)/ 0.15567 (neutral)/ 0.2 (stable)
Number of popping attempts	1000	1000
Number of popped turbines	10	10

The EPS for the offshore case is compared to an Adapted Genetic Algorithm [19]. The wind case used is of unidirectional wind direction and a single wind speed of 12 m/s approaching from the bottom of the field (Fig. 4). Since the wind speed and direction are constant, efficiency is simplified and can be determined using Equation 19:

$$\eta = \frac{P_{tot}}{N \times P(u)} \tag{19}$$

where P_{tot} is the total power produced by the farm, and $P(u)$ is the power produced by each turbine when the wind speed at the rotor is equal to the ambient wind speed, 12 m/s. The farm area is a square with side lengths equal to 4000 m. The rated wind speed for each turbine is 14 m/s and rated power is fixed at 5 MW. Rotor radius is calculated to be 43.5 m, and hub height is not given, but will assumed to be equal to 90 m (Table 2).

TABLE 2: EPS AND ADAPTED GA COMPARISON PARAMETERS

Ambient wind speed	Rated wind speed	Rated power	Grid size	Hub Height
12 m/s	14 m/s	5 MW	4 km x 4 km	90 m

5. RESULTS

Layouts were optimized for farms containing between 15 and 60 turbines for both onshore and offshore environments based on parameters given in Table 1. Each set was generated five times. The relationship between number of turbines and the objective function is quadratic for the offshore environment (Fig. 5, $R^2 = 0.5597$) and cubic for the onshore environment (Fig. 6, $R^2 = 0.3909$). The hub height and rotor radius of each turbine are indicated the key given in Fig. 7. The offshore environment has a minimum objective evaluation when the layout is optimized for 42 turbines; the minimum objective evaluation for a 42 turbine layout is -1.79456e+08 (Fig. 8). The cost of cabling for the 42 turbine layout is approximately $1.9432e+7, resulting in an objective function evaluation equal to -1.60024e+08 (Table 3). The onshore environment has a minimum objective evaluation when the layout is optimized for 32 turbines; the minimum objective evaluation for a 32 turbine layout is -1.64933e+08 (Fig. 9).

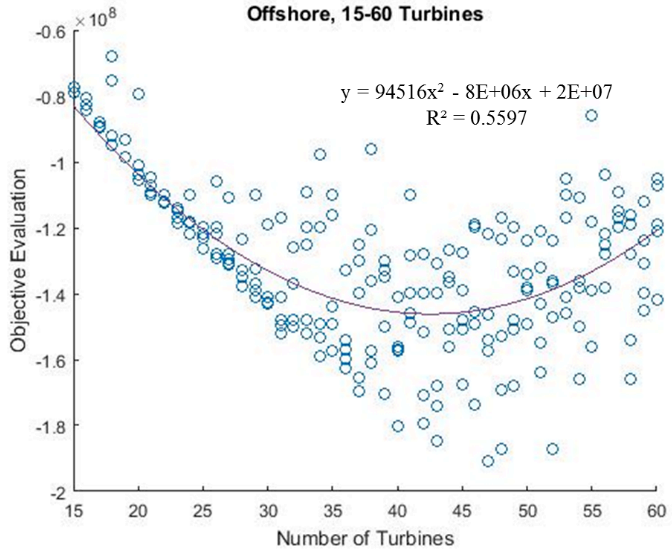

FIGURE 5: OBJECTIVE EVALUATION FOR OFFSHORE LAYOUTS CONTAINING 15 TO 60 TURBINES

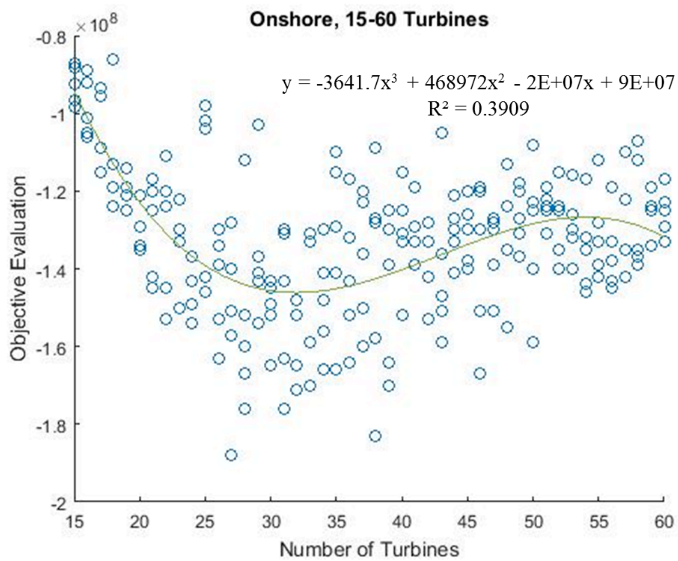

FIGURE 6: OBJECTIVE EVALUATION FOR ONSHORE LAYOUTS CONTAINING 15 TO 60 TURBINES

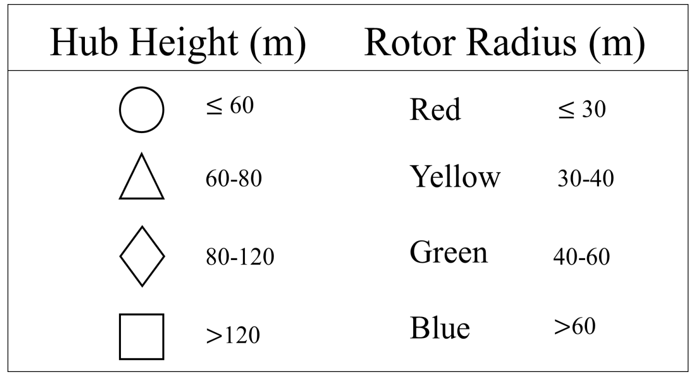

FIGURE 7: TURBINE GEOMETRY KEY

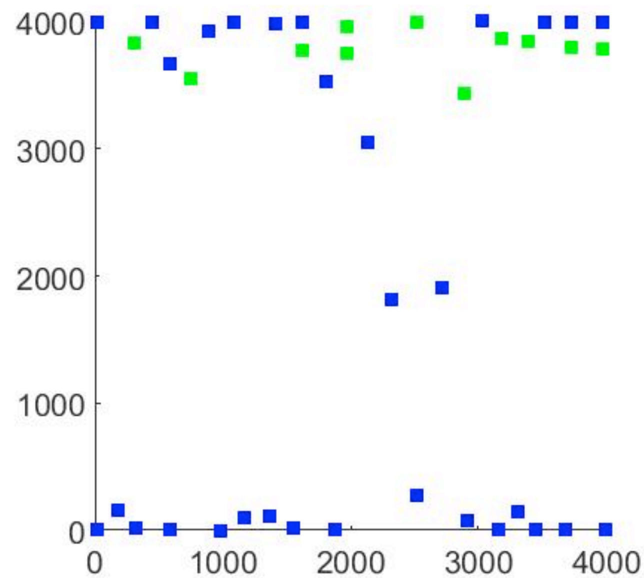

FIGURE 8: 42 TURBINE OFFSHORE LAYOUT, OBJECTIVE EVALUATION = -1.79456e+08

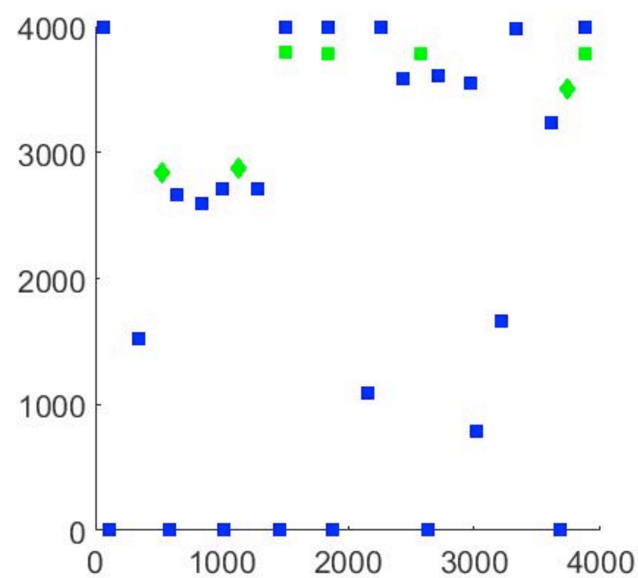

FIGURE 9: 32 TURBINE ONSHORE LAYOUT, OBJECTIVE EVALUATION = -1.64933e+08

TABLE 3: MINIMUM OBJECTIVE EVALUATIONS FOR OFFSHORE AND ONSHORE LAYOUTS

	Offshore	Onshore
Optimal Number of Turbines	42	32
Minimum Objective Evaluation	-1.79456e+08 (-1.60024e+08)	-1.64933e+08
R^2 Value	0.5597	0.3909

Layouts were optimized for an offshore environment based on parameters given in Table 2. A 16-turbine layout was generated using the EPS and compared to the layout generated using the Adapted GA [19] (Figures 10 and 11). Efficiencies (Eq. 19) for layouts containing between 15 and 60 turbines are shown in Fig. 7. Layouts generated by the EPS are 100% efficient up to 34 turbines (Fig. 13).

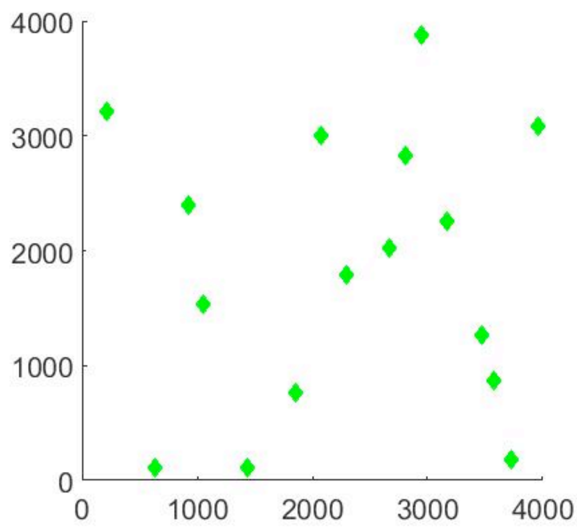

FIGURE 10: 16 TURBINE LAYOUT, EPS, 100% EFFICIENCY

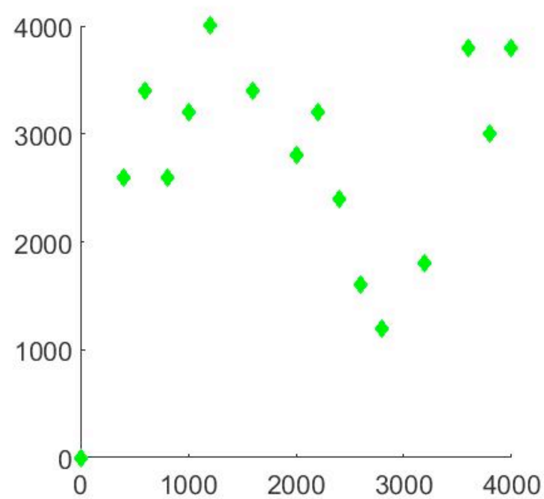

FIGURE 11: 16 TURBINE LAYOUT, ADAPTED GA, 100% EFFICIENCY (Liu and Wang [19])

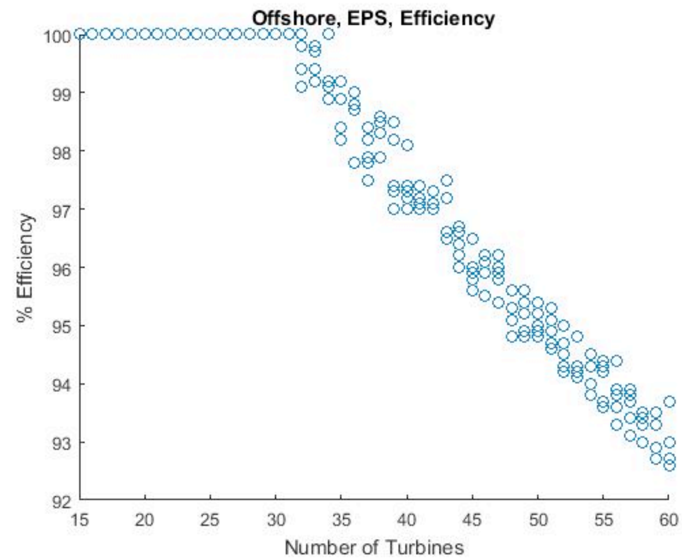

FIGURE 12: EFFICIENCY OF EPS-GENERATED LAYOUTS

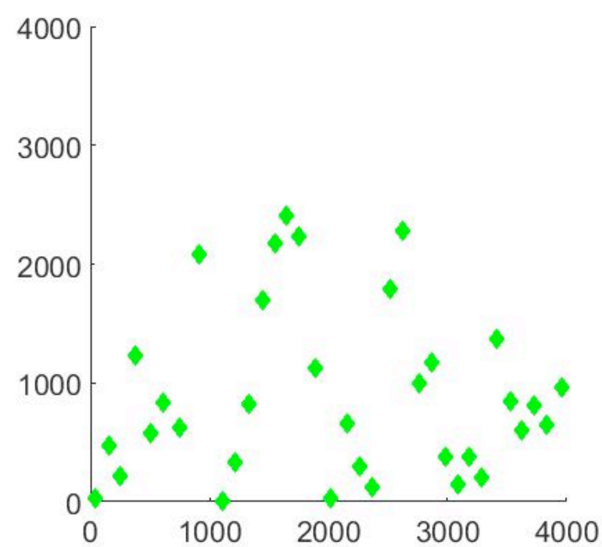

FIGURE 13: 34 TURBINE LAYOUT, EPS, 100% EFFICIENCY

6. DISCUSSION

The deviation in the optimal number of turbines between the onshore and offshore minimum objective evaluations can be attributed to three differences: cost, surface roughness, and power law exponent. The surface roughness and power law exponents for both onshore and offshore environments are given in Table 1. These values affect the wind speed with respect to elevation and the shape of a wake behind a rotor. Changing these values affects where the EPS places turbines in reference to other turbines, since the turbine agents try to avoid being placed in wakes. However, the change in cost more greatly affects the optimal number of turbines as evaluated by the objective function. Higher investment in offshore wind farms are required for them to be as profitable as onshore wind farms due to higher initial costs. However, results from this work indicate that offshore wind farms may be as profitable as onshore wind farms over a 20-year lifetime. It should be noted that the cost model used in this work is new, and it has inherent uncertainty that propagates throughout the execution of the optimization algorithm. That, coupled with the relative simplicity of the indicated wind cases (unidirectional, single-wind-speed) limit the real-world applicability of the current method. Objective evaluations determined in this work may not represent actual profit margins for real wind farms; however, subsequent improvement to the utilized modeling will be conducted to improve accuracy.

The layouts shown in Figures 8 and 9 contain large turbines populating the front and back of the field, with turbines scattered throughout the middle of the field. The turbines at the front of the field are unaffected by wakes, and are able to extract the most energy from the ambient wind speed. The turbines at the far back of the field have spread out in order to move far away from the wakes of upstream turbines; this is commonly seen in optimized wind farm layouts [26–29]. For the offshore layout, most turbines are within the largest rotor radius and hub height group, indicating that the power they are able to generate outweighs the increase in cost caused by the increased size of the turbines. The layouts shown in Figs. 9 and 10 are selected based on their objective evaluations; it is important to note that the common behavior across layouts are shown in these figures, but it may be possible to improve the location of individual turbines.

The noise in the data for both the onshore and offshore objective evaluations is due to the randomness of the EPS (Figs. 14 and 15). The three stochastic extensions help to avoid settling on poor-performing local optima. However, factors such as poor initial layouts or insufficient popping attempts can lead to variation in the objective evaluation for layouts containing the same number of turbines.

The efficiency of the 16 turbine layouts for both the Adapted GA and EPS are 100%. However, this may be attributable to the large area of the farm; turbines are able to easily spread out at this size to reach optimal efficiency. As the number of turbines in the farm increases, the more difficult it becomes for the farm to be theoretically perfectly efficient. Layouts with more than 16 turbines are not provided for the Adapted GA, therefore, the greatest number of turbines in a farm at 100% efficiency cannot be compared to the EPS [19]. However, the Adapted GA requires the field area to be discretized into 200 m by 200 m sections, limiting the number of possible layout solutions. The EPS is able to optimize continuously within the field area such that a greater number of highly efficient layouts are possible.

7. CONCLUSION

An EPS approach is presented that has been applied to the optimization of floating offshore wind farm layouts. Cost is minimized while power is maximized in order to maximize profitability. Three advanced models are incorporated to properly represent the cost, power production, and wake interactions for floating offshore wind farms.

Results from the offshore wind farm layouts are compared to similarly-optimized onshore wind farm layouts. It is discovered that comparable objective evaluations can be achieved for both the onshore and offshore layouts for farms containing a different number of turbines. While investment costs for offshore wind farms are much higher than onshore wind farms, over a life of 20 years they can achieve comparable profitability given the current problem formulation and modeling. In addition, while increasing the size of wind turbines increases investment costs, the offshore layouts chose to implement large turbine sizes, indicating that the power produced over the life of the farm will offset higher investment costs.

The EPS is compared to resulting layouts obtained using an Adapted GA. For 16-turbine layouts, both the EPS and Adapted GA generated 100% efficient layouts. The EPS also generated 100% efficient layouts for farms containing twice as many turbines as the layout presented by the Adapted GA.

ACKNOWLEDGMENTS

This work has been funded by Oregon State University.

REFERENCES

[1] Martin, L., 2014, "Lower U.S. electricity demand growth would reduce fossil fuels' projected generation share," EIA.

[2] Lindenberg, S., Smith, B., and O'Dell, K., 2008, 20% Wind energy by 2030, Washington, DC.

[3] Schwartz, M., Heimiller, D., Haymes, S., and Musial, W., 2010, Assessment of Offshore Wind Energy Resources for the United States, Golden, Colorado.

[4] Breton, S. P., and Moe, G., 2009, "Status, plans and technologies for offshore wind turbines in Europe and North America," Renew. Energy.

[5] Sclavounos, P. D., Tracy, C., and Lee, S., 2007, "Floating Offshore Wind Turbines: Responses in a Seastate, Pareto Optimal Designs and Economic Assessment," Int. Conf. Offshore …, pp. 1–20.

[6] Sclavounos, P., 2008, "Floating Offshore Wind Turbines," Mar. Technol. Soc. J., **42**(2), pp. 39–43.

[7] Byrne, B. W., and Houlsby, G. T., 2003, "Foundations for offshore wind turbines.," Philos. Trans. A. Math. Phys. Eng. Sci.

[8] Roddier, D., Cermelli, C., Aubault, A., and Weinstein, A., 2010, "WindFloat: A floating foundation for offshore wind turbines," J. Renew. Sustain. Energy, **2**, pp. 1–34.

[9] Carrington, D., 2014, "Drifting off the coast of Portugal, the frontrunner in the global race for floating wind farms," Guard.

[10] 2014, "Marine Transmission in Oregon Oregon Department of Energy Marine Transmission in Oregon Marine Transmission in Oregon Report to Oregon Legislature."

[11] Principle Power, 2014, "U.S. Department of Energy Supports Oregon Offshore Wind with Grant Accelerating Development of WindFloat Pacific Project," p. Press Release.

[12] Elkinton, C. N., Manwell, J. F., and McGowan, J. G., 2005, "Offshore Wind Farm Layout Optimization (OWFLO) Project: An Introduction," Optimization.

[13] Elkinton, C. N., Manwell, J. F., and McGowan, J. G., 2008, "Algorithms for Offshore Wind Farm Layout," Wind Eng., **32**(1), pp. 67–83.

[14] Pérez, B., Mínguez, R., and Guanche, R., 2013, "Offshore wind farm layout optimization using mathematical programming techniques," Renew. Energy.

[15] Gao, X., Yang, H., and Lu, L., 2014, "Investigation into the optimal wind turbine layout patterns for a Hong Kong offshore wind farm," Energy, **73**(June 2015), pp. 430–442.

[16] Gao, X., Yang, H., Lin, L., and Koo, P., 2015, "Wind turbine layout optimization using multi-population genetic algorithm and a case study in Hong Kong offshore," J. Wind Eng. Ind. Aerodyn., **139**, pp. 89–99.

[17] Szafron, C., 2010, "Offshore windfarm layout optimization," 2010 9th Conf. Environ. Electr. Eng. EEEIC 2010, pp. 542–545.

[18] Réthoré, P. E., Fuglsang, P., Larsen, G. C., Buhl, T., Larsen, T. J., and Madsen, H. a., 2013, "TOPFARM: Multi-fidelity optimization of offshore wind farms," Wind Energy, (DECEMBER).

[19] Liu, F., and Wang, Z., 2014, "Offshore Wind Farm Layout Optimization Using Adapted Genetic Algorithm: A different perspective."
[20] Rivas, R. A., Clausen, J., Hansen, K. S., and Jensen, L. E., 2009, "Solving the Turbine Positioning Problem for Large Offshore Wind Farms by Simulated Annealing," Wind Eng., **33**(3), pp. 287–297.
[21] Ituarte-Villarreal, C. M., and Espiritu, J. F., 2011, "Optimization of wind turbine placement using a viral based optimization algorithm," Procedia Comput. Sci., **6**, pp. 469–474.
[22] Mosetti, G., Poloni, C., and Diviacco, B., 1994, "Optimization of wind turbine positioning in large windfarms by means of a genetic algorithm," J. Wind Eng. Ind. Aerodyn., **51**(1), pp. 105–116.
[23] Salcedo-Sanz, S., Gallo-Marazuela, D., Pastor-Sánchez, A., Carro-Calvo, L., Portilla-Figueras, A., and Prieto, L., 2014, "Offshore wind farm design with the Coral Reefs Optimization algorithm," Renew. Energy.
[24] Rodrigues, S. F., Teixeira Pinto, R., Soleimanzadeh, M., Bosman, P. a. N., and Bauer, P., 2015, "Wake losses optimization of offshore wind farms with moveable floating wind turbines," Energy Convers. Manag., **89**, pp. 933–941.
[25] Guérivière, P. de la, 2011, Press Release: IDEOL Announces a New Floating Platform Solution to Accelerate the Deployment of Offshore Wind Farms, La Ciotat, France.
[26] DuPont, B., Cagan, J., and Moriarty, P., 2015, "AN ADVANCED MODELING SYSTEM FOR OPTIMIZATION OF WIND FARM LAYOUT AND WIND TURBINE SIZING USING A MULTI-LEVEL EXTENDED," Energy, **In Press**, pp. 1–26.
[27] DuPont, B. L., and Cagan, J., 2012, "An Extended Pattern Search Approach to Wind Farm Layout Optimization," ASME J. Mech. Des., **134**, pp. 1–18.
[28] DuPont, B. L., and Cagan, J., 2013, "Multi-Stage Optimization of Wind Farms with Limiting Factors," ASME Int. Des. Eng. Tech. Conf. Comput. Inf. Eng. Conf., pp. 1–12.
[29] DuPont, B. L., Cagan, J., and Moriarty, P., 2012, "Optimization of Wind Farm Layout and Wind Turbine Geometry Using a Multi-Level Extended Pattern Search Algorithm That Accounts for Variation in Wind Shear Profile Shape," Volume 3: 38th Design Automation Conference, Parts A and B, Chicago, Illinois, USA, p. 243.
[30] Hooke, R., and Jeeves, T. A., 1961, ""Direct Search'' Solution of Numerical and Statistical Problems," J. ACM, **8**(2), pp. 212–229.
[31] Torczon, V., 1995, "Pattern Search Methods for Nonlinear Optimization," SIAG/OPT Views News, **6**, pp. 7–11.
[32] Yin, S., and Cagan, J., 2000, "An Extended Pattern Search Algorithm for 3D Component Layout."
[33] Manwell, J. F., McGowan, J. G., and Rogers, A. L., 2009, Wind Energy Explained: theory, design, and application, John Wiley & Sons Ltd., West Sussex, UK.
[34] Jensen, N. O., 1983, "A Note on wind generator interaction," Risø-M, p. 16.
[35] Jonkman, J., Butterfield, S., Musial, W., and Scott, G., 2009, "Definition of a 5-MW reference wind turbine for offshore system development," Contract, (February), pp. 1–75.
[36] Castro-Santos, L., and Diaz-Casas, V., 2014, "Life-cycle cost analysis of floating offshore wind farms," Renew. Energy, **66**, pp. 41–48.
[37] Myhr, A., Bjerkseter, C., Ågotnes, A., and Nygaard, T. a., 2014, "Levelised cost of energy for offshore floating wind turbines in a life cycle perspective," Renew. Energy, **66**, pp. 714–728.
[38] Castro-Santos, L., Ferreño González, S., and Diaz-Casas, V., 2013, "Methodology to calculate mooring and anchoring costs of floating offshore wind devices," International Conference on Renewable Energies and Power Quality (ICREPQ)1, Bilbao.
[39] Castro-Santos, L., and Diaz-Casas, V., 2015, "Economic influence of location in floating offshore wind farms," Ocean Eng., **107**, pp. 13–22.
[40] 2011, "WindFloat" [Online]. Available: www.principlepowerinc.com.
[41] Lantz, E., Goldberg, M., and Keyser, D., 2013, "Jobs and Economic Development Impact (JEDI) Model: Offshore Wind User Reference Guide," (June).
[42] Baker, C., 2015, "Substation Costs."
[43] 2015, "Burea of Ocean Energy Management," Dep. Energy.
[44] 2012, Commercial Lease of Submerged Lands for Renewable Energy Development on the Outer Continental Shelf, Herndon, VA.
[45] Hsu, S. a., Meindl, E. a., and Gilhousen, D. B., 1994, "Determining the power-law wind-profile exponent under near-neutral stability conditions at sea," Am. Meteorol. Soc., pp. 757–765.